PHYSICAL REVIEW E **80**, 061115 (2009)

Molecular wires acting as quantum heat ratchets

Fei Zhan,[1,*] Nianbei Li,[1,†] Sigmund Kohler,[2,‡] and Peter Hänggi[1,3,§]
[1]*Institut für Physik, Universität Augsburg, Universitätsstr. 1, D-86135 Augsburg, Germany*
[2]*Instituto de Ciencia de Materiales de Madrid, CSIC, Cantoblanco, E-28049 Madrid, Spain*
[3]*Department of Physics and Centre for Computational Science and Engineering, National University of Singapore, Singapore 117542, Republic of Singapore*

(Received 15 September 2009; published 14 December 2009)

We explore heat transfer in molecular junctions between two leads in the absence of a finite net thermal bias. The application of an unbiased time-periodic temperature modulation of the leads entails a dynamical breaking of reflection symmetry, such that a directed heat current may emerge (ratchet effect). In particular, we consider two cases of adiabatically slow driving, namely, (i) periodic temperature modulation of only one lead and (ii) temperature modulation of both leads with an ac driving that contains a second harmonic, thus, generating harmonic mixing. Both scenarios yield sizable directed heat currents, which should be detectable with present techniques. Adding a static thermal bias allows one to compute the heat current-thermal load characteristics, which includes the ratchet effect of negative thermal bias with positive-valued heat flow against the thermal bias, up to the thermal stop load. The ratchet heat flow in turn generates also an electric current. An applied electric stop voltage, yielding effective zero electric current flow, then mimics a solely heat-ratchet-induced thermopower ("ratchet Seebeck effect"), although no net thermal bias is acting. Moreover, we find that the relative phase between the two harmonics in scenario (ii) enables steering the net heat current into a direction of choice.

DOI: 10.1103/PhysRevE.80.061115 PACS number(s): 05.40.−a, 44.10.+i, 63.22.−m, 05.60.Gg

I. INTRODUCTION

In recent years, we have witnessed the development of nanodevices based on molecular wires [1–5]. One of their essential features is that the electric current through them can be controlled effectively. One approach to such transport control is based on conformational changes in the molecule [6–8]. Another scheme relies on the dipole interaction between the molecular wire and a tailored laser field [9–13]. A further approach employs gate voltages acting on the wire [14–16]. The latter allows a transistorlike control, which has already been demonstrated experimentally [17–19]. It is therefore interesting to explore as well the related control of heat transport.

In general, heat transport through a molecular junction involves the combined effect of electron as well as phonon transfer processes. Control of phonon transport is much more complicated since the phonon number is not conserved. Nevertheless, the field of phononics, i.e., control and manipulation of phonons in nanomaterials, has emerged [20]. This includes functional devices, such as thermal diodes [21–27], thermal transistors [28,29], thermal logic gates [30], and thermal memories [31] based on the presence of a static temperature bias. The corresponding theoretical research has been accompanied by experimental efforts on nanosystems. In particular, solid-state thermal diodes have been realized with asymmetric nanotubes [32] and with semiconductor quantum dots [33].

Upon harvesting ideas from the field of Brownian motors [34–38]—originally devised for particle transport—a classical Brownian *heat engine* has been proposed to rectify and steer heat current in nonlinear lattice structures [39,40]. In the absence of any static nonequilibrium bias, a nonvanishing net heat flow can be induced by unbiased temporally alternating bath temperatures combined with nonlinear interactions among neighboring lattice sites. This so obtained directed heat current can be readily controlled to reverse direction. If, in addition, a thermal bias across the molecule is applied, a heat current can then be directed even against an external thermal bias. This setup is therefore rather distinct from adiabatic and nonadiabatic electron heat pumps, which involve photon-assisted transmission and reflection processes in the presence of irradiating photon sources [4,41,42].

In this work, we investigate the possibility of steering heat through a molecular junction in the presence of a gating mechanism. In our model, the bath temperatures of adjacent leads are subjected to slow time-periodic modulations. Both the electronic and the phononic heat current are considered, as is sketched in Fig. 1. A finite directed ratchet heat current requires breaking reflection symmetry. This can be achieved by spatial asymmetries in combination with nonequilibrium fields [34–38] or in a purely dynamical way [43–47]. We

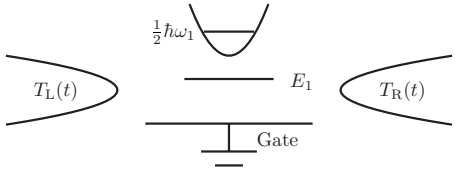

FIG. 1. Setup of a molecular junction whose electronic level E_1 can be gated, while the vibrational frequency ω_1 is fixed. The lead temperatures $T_{\rm L}({\rm R})(t)$ are subjected to time-periodic modulations.

*fei.zhan@physik.uni-augsburg.de
†nianbei.li@physik.uni-augsburg.de
‡sigmund.kohler@icmm.csic.es
§hanggi@physik.uni-augsburg.de

focus on an unbiased temporal temperature variation in the connecting leads. While the prior studies of Refs. [39,40] deal with classical heat transport across nonlinear lattices, our focus here is on the of *quantum* heat-ratchet effect in a molecular wire system, originating from both phonons and electrons. Owing to the modulation of temperature in the connecting leads (see Fig. 1), our analysis demonstrates the controllability of the emerging ratchet heat current.

This paper is organized as follows. In Sec. II, we specify the physical assumptions and introduce our model together with the basic theoretical concepts for directing heat current across a short gated molecular junction formed by a harmonically oscillating molecule. The heat flux is induced by temperature modulations in the contacting leads. Section III presents the results for case (i) where the temperature is modulated in one lead only. We elaborate on pumping heat against a static thermal bias and consider the resulting thermoelectric power. In Sec. IV, we consider case (ii) in which both lead temperatures are periodically but asymmetrically modulated. A finite directed heat current emerges from harmonic mixing of different frequencies, which entails dynamical symmetry breaking. Since the leading order of this heat current is the third order in the driving amplitude, the overall rectification is weaker as compared to case (i) where the heat flux starts out at second order in the driving amplitude. The latter scheme with its symmetric static parameters, however, provides a more efficient control scenario. The direction of the resulting heat current can be readily reversed either by a gate voltage or by adjusting the relative phase shift within the harmonic mixing signal for the temperature modulation. Section V contains a summary and an outlook.

II. PHYSICAL ASSUMPTIONS, MODEL, AND BALLISTIC HEAT TRANSFER

We consider a molecular junction between two leads, where a static gate voltage acting on the junction. Heat transport from both electrons and phonons is taken into account. Since we focus on coherent transport in a short molecular wire [48–50], electron-phonon interaction can be ignored. Moreover, we treat ballistic heat transfer for the electron system and the phonon system in the absence of anharmonic interactions and dissipative intrawire scattering processes. Then, the heat flux can be obtained in terms of a Landauer-type expression involving corresponding temperature-independent transmission probabilities for both the electrons [51,52] and the phonons [54,55]. The total Hamiltonian can thus be separated into electron and phonon parts, i.e.,

$$H = H^{\mathrm{el}} + H^{\mathrm{ph}}, \tag{1}$$

each of which consisting of a wire contribution, a lead contribution, and an interaction term, such that

$$H^{\mathrm{el}}(\mathrm{ph}) = H^{\mathrm{el(ph)}}_{\mathrm{wire}} + H^{\mathrm{el(ph)}}_{\mathrm{leads}} + H^{\mathrm{el(ph)}}_{\mathrm{contacts}}. \tag{2}$$

The short molecular wire is modeled as a single energy level and one harmonic phonon mode only. Then the Hamiltonian of the wire electron in tight-binding approximation reads as

$$H^{\mathrm{el}}_{\mathrm{wire}} = E_1 |1\rangle\langle 1|, \tag{3}$$

where E_1 describes the on-site energy of the tight-binding level, which can be shifted via a gate voltage. The electrons in the leads are modeled as ideal electron gases, i.e.,

$$H^{\mathrm{el}}_{\mathrm{leads}} = H_{\mathrm{L}} + H_{\mathrm{R}} = \sum_q \epsilon_{\mathrm{L}q} c^\dagger_{\mathrm{L}q} c_{\mathrm{L}q} + \sum_q \epsilon_{\mathrm{R}q} c^\dagger_{\mathrm{R}q} c_{\mathrm{R}q}, \tag{4}$$

where $c^\dagger_{lq}$ creates an electron in state $|lq\rangle$ of lead $l=\mathrm{L},\mathrm{R}$. The electron-tunneling Hamiltonian

$$H^{\mathrm{el}}_{\mathrm{contacts}} = \sum_q (V_{\mathrm{L}q} c^\dagger_{\mathrm{L}q} c_1 + V_{\mathrm{R}q} c^\dagger_{\mathrm{R}q} c_1) + \mathrm{H.c.} \tag{5}$$

establishes the contact between the wire and the leads. This tunneling coupling is characterized by the spectral density $\Gamma_l(\epsilon) = 2\pi\Sigma_q |V_{lq}|^2 \delta(\epsilon - \epsilon_{lq})$. We assume symmetric coupling within a wide-band limit such that $\Gamma_l(\epsilon) = \Gamma$.

The phonon mode is represented by a harmonic oscillator with the Hamiltonian

$$H^{\mathrm{ph}}_{\mathrm{wire}} = \frac{P^2}{2M} + \frac{1}{2} M \omega_1^2 Q^2, \tag{6}$$

where Q and P denote the position and the momentum operator, respectively, M denotes the atom mass, and ω_1 is the characteristic phonon frequency of wire. Following the reasoning put forward in Ref. [55], the two phonon baths and its bilinear coupling to the wire system are described by

$$H^{\mathrm{ph}}_{\mathrm{leads}} + H^{\mathrm{ph}}_{\mathrm{contacts}} = \sum_{l,k} \left\{ \frac{p^2_{lk}}{2m_l} + \frac{m_l \omega^2_{lk}}{2} \left(x_{lk} - \frac{g_l Q}{m_l \omega_{lk}} \right)^2 \right\}, \tag{7}$$

where x_{lk}, p_{lk}, ω_{lk} are the position operators, momentum operators, and frequencies associated with the bath degrees of freedom; m_l are the masses and $g_l = g_{\mathrm{L}} = g_{\mathrm{R}} = g$ represent a symmetric phonon wire-lead coupling strength for lead $l=\mathrm{L},\mathrm{R}$. The position and momentum operators can be expressed in terms of the creation and annihilation operators for phonons as $x_{lk} = \sqrt{\hbar/2m_l\omega_{lk}}(a^\dagger_{lk} + a_{lk})$ and $p_{lk} = i\sqrt{\hbar m_l \omega_{lk}/2}(a^\dagger_{lk} - a_{lk})$.

Henceforth, we assume that the temperature modulations acting on the baths are always sufficiently slow so that the leads are always at thermal quasiequilibrium for the molecular wire. The heat transport then obeys the adiabatic coherent quantum transport laws, as discussed below [see Eqs. (13) and (14)].

A. Adiabatic modulation of the lead temperatures

At thermal equilibrium with temperature $T = T_{\mathrm{L}} = T_{\mathrm{R}}$ with equal electrochemical potentials $\mu_{\mathrm{L}} = \mu_{\mathrm{R}} = \mu$, the density matrix for the leads reads as $\rho_l \propto \exp\{-(H^{\mathrm{ph}}_l + H^{\mathrm{el}}_l - \mu_l N_l)/k_{\mathrm{B}} T_l\}$, where $N_l = \Sigma_q c^\dagger_{lq} c_{lq}$ is the number of electrons in lead $l=\mathrm{L},\mathrm{R}$ and $k_{\mathrm{B}} T_l$ denotes the present lead temperature multiplied by the Boltzmann constant. To induce shuttling of heat, we invoke a nonequilibrium situation via an adiabatically slow temperature modulation $T_l(t)$ in the leads. The latter can be realized experimentally, for example, by use of a heating/cooling circulator [57]. Then the expectation values of the electron and phonon lead operators read as

$$\langle c^{\dagger}_{l'q'} c_{lq} \rangle = f_l[\epsilon_q, T_l(t)] \delta_{ll'} \delta_{qq'}, \tag{8}$$

$$\langle a^{\dagger}_{l'k'} a_{lk} \rangle = n_l[\omega_k, T_l(t)] \delta_{ll'} \delta_{kk'}, \tag{9}$$

where $f_l[\epsilon, T_l(t)] = \{\exp[(\epsilon - \mu_l)/k_B T_l(t)] + 1\}^{-1}$ and $n_l[\omega, T_l(t)] = \{\exp[\hbar\omega/k_B T_l(t)] - 1\}^{-1}$ denote the Fermi-Dirac distribution and the Bose-Einstein distribution, respectively, which both inherit a time dependence from the temperature modulation. This implies a time-scale separation, which is justified because for laser heating of a metallic system, the electrons undergo rather fast thermalization [58–61]. The corresponding relaxation times stem from electron-electron and electron-phonon interaction and for a typical metal is in the order of a few fs or ps, respectively [62,63]. The assumption of adiabatically slow temperature modulation requires that the driving frequency is smaller than the reciprocal of the larger time scale, i.e., $\Omega \ll (1\ \text{ps})^{-1} = 1\ \text{THz}$.

The lead temperatures $T_L(t)$ and $T_R(t)$ are assumed to vary time periodically $T_{L(R)}(t) = T_{L(R)}(t + 2\pi/\Omega)$, where the time average $T_0 = \overline{T_L(t)} = \overline{T_R(t)}$ marks the environmental reference temperature. This implies a vanishing temperature bias

$$\overline{\Delta T(t)} \equiv \overline{T_L(t) - T_R(t)} = 0. \tag{10}$$

In the long-time limit, the time-dependent asymptotic heat current $J_Q(t) = J_Q^{\text{el}}(t) + J_Q^{\text{ph}}(t)$ assumes the periodicity $2\pi/\Omega$ of the external driving field

$$J_Q(t) = J_Q(t + 2\pi/\Omega). \tag{11}$$

Henceforth, we focus on the stationary heat current $\overline{J_Q}$, which follows from the average over a full driving period:

$$\overline{J_Q} = \frac{\Omega}{2\pi} \int_0^{2\pi/\Omega} J_Q(t) dt. \tag{12}$$

If the lead temperatures are modulated slowly enough (adiabatic temperature rocking), the dynamical thermal bias $\Delta T(t)$ can be viewed as a static bias at time t in the adiabatic limit $\Omega \to 0$. Thus, the asymptotic electron and phonon heat currents $J_Q^{\text{el(ph)}}(t)$ can be expressed by the Landauer-type formula for electron heat flux [51,52] and for the phonon heat flux [53–56], such that

$$J_Q^{\text{el}}(t) = \frac{1}{2\pi\hbar} \int_{-\infty}^{\infty} d\varepsilon (\varepsilon - \mu) \mathcal{T}^{\text{el}}(\varepsilon) \{f[\varepsilon, T_L(t)] - f[\varepsilon, T_R(t)]\}, \tag{13}$$

$$J_Q^{\text{ph}}(t) = \frac{1}{2\pi} \int_0^{\infty} d\omega \hbar\omega \mathcal{T}^{\text{ph}}(\omega) \{n[\omega, T_L(t)] - n[\omega, T_R(t)]\}, \tag{14}$$

where $\mathcal{T}^{\text{el}}(\varepsilon)$ and $\mathcal{T}^{\text{ph}}(\omega)$ denote the temperature-independent transmission coefficients for electrons with energy ε and phonons with frequency ω scattered from the left lead to the right lead, respectively. Note that the two opposite heat fluxes are not at equilibrium with each other and that the heat energy transferred by a single electron-scattering process is $\varepsilon - \mu$ rather than ε [41]. The reason for this is the following. At zero temperature, where the energy levels below Fermi energy μ are fully occupied, no heat current is transferred since no electron can tunnel. At finite temperatures, the tunneling process is thermally activated. An electron with energy ε tunneling from left lead to right lead will dissipate to the Fermi energy level. Therefore, the heat energy transferred by this electron is $\varepsilon - \mu$.

The electron transmission coefficient $\mathcal{T}^{\text{el}}(\varepsilon)$ can be expressed by the electron Green's functions [4]

$$\mathcal{T}^{\text{el}}(\varepsilon) = \text{Tr}[G^{\dagger}(\varepsilon) \Gamma^{R} G(\varepsilon) \Gamma^{L}], \tag{15}$$

where $\Gamma^l = |1\rangle \Gamma_l \langle 1|$ stems from the tunnel coupling to lead $l = L, R$. For the present case of a one-site wire, this operator is simply a 1×1 matrix, so that the Green's function reads as

$$G(\varepsilon) = \frac{|1\rangle\langle 1|}{\varepsilon - (E_1 - i\Gamma)}, \tag{16}$$

where $\Gamma = \frac{1}{2}(\Gamma_L + \Gamma_R)$.

For a molecular wire with a single level, such as described by Eq. (3), the electron transmission assumes Breit-Wigner form and reads as [4]

$$\mathcal{T}^{\text{el}}(\varepsilon) = \frac{\Gamma^2}{(\varepsilon - E_1)^2 + \Gamma^2}, \tag{17}$$

where we have assumed symmetric electron wire-lead coupling such that $\Gamma = \Gamma_L = \Gamma_R$.

The phonon transmission coefficient $\mathcal{T}^{\text{ph}}(\omega)$ is evaluated following Ref. [55]. As is shown in the Appendix, it assumes for one phonon mode a Breit-Wigner form as well, i.e., the temperature-independent phonon transmission probability reads as

$$\mathcal{T}^{\text{ph}}(\omega) = \frac{4\omega^2 \gamma^2(\omega)}{(\omega^2 - \omega_1^2)^2 + 4\omega^2 \gamma^2(\omega)}, \tag{18}$$

where $\gamma(\omega) = a e^{-\omega/\omega_D}$. Here ω_D is the Debye cut-off frequency of phonon reservoirs in the lead and $a = \pi g^2 / 4mM\omega_D^3$ incorporates the phonon wire-lead coupling $g = g_L = g_R$.

B. Experimental parameters and physical time scales

In our numerical investigation, we insert the electron wire-lead tunnel rate $\Gamma = 0.11$ eV, which has been used also to describe electron tunneling between a phenyldithiol molecule and gold contact [64]. The phonon frequency $\omega_1 = 1.4 \times 10^{14}\ \text{s}^{-1}$ is typical for a carbon-carbon bond [65]. For the Debye cut-off frequency of the phonon reservoirs, we use the value for gold, which is $\omega_D = 2.16 \times 10^{13}\ \text{s}^{-1}$. The phonon coupling frequency $a = 1.04 \times 10^{15}\ \text{s}^{-1}$ is chosen such that the static thermal conductance assumes the value 50 pWK^{-1}, which has been measured in experiments with alkane molecular junctions [66].

These parameters imply physical time scales, which are worth being discussed. During the dephasing time, electron-phonon interactions within the wire destroy the electron's quantum-mechanical phase. If this time is larger than the dwell time, i.e., the time an electron spends in the wire, the electron transport is predominantly coherent [48]. Following Ref. [48], we estimate the dwell time by the tunneling tra-

versal time $\tau \sim \hbar[(E_1-\mu)^2+\Gamma^2]^{-1/2}$, which for our parameters is on the order $\tau \sim 5$ fs and, thus, much shorter than the typical electron-phonon relaxation time (dephasing time), which is on the order of 1 ps. This implies that the electron-phonon interaction also does not affect the electron coherence and can be ignored. Another important time scale is the phonon lifetime for escaping into the corresponding lead and can be estimated as $1/a \sim 1$ fs. Among the above-mentioned time scales, the maximum time scale is the electron-phonon relaxation time, which is in the order of ps. Thus, the regime of validity of our assumption for adiabatic temperature modulations is justified when the angular driving frequency is much slower than the electron-phonon relaxation rate within lead, i.e., $\Omega \ll 1$ THz.

III. PUMPING HEAT VIA SINGLE-SIDED TEMPERATURE ROCKING

Let us first consider the case in which the temperature of one lead is modulated harmonically, while the temperature of the other lead is constant,

$$T_{\mathrm{L}}(t) = T_0 + A\cos(\Omega t),$$

$$T_{\mathrm{R}}(t) = T_0. \tag{19}$$

Here A and Ω are the amplitude and the (angular) frequency of the temperature modulation, respectively, while T_0 is the reference temperature. The driving amplitude A is positive and bounded by the temperature T_0 since $T_{\mathrm{L}}(t)$ has to remain positive at any time. The temperature difference between the left lead and the right lead reads as $\Delta T(t)=A\cos(\Omega t)$, such that the net thermal bias vanishes on time average $\overline{\Delta T(t)}=0$. Unless mentioned explicitly otherwise, we use unbiased source-drain leads with the chemical potentials being $\mu_L = \mu_R = \mu$, i.e., there is no voltage bias acting.

The cycle-averaged heat fluxes, both the electronic and the phononic one, follow from numerically evaluating the integrals in Eqs. (13) and (14). As expected for an adiabatic theory, we observe that the average heat current $\overline{J_Q}$ is independent of the driving frequency Ω. This is in accordance with the findings for ballistic heat transfer in the adiabatic regime.

In an experiment, the molecular level E_1 can be manipulated by a gate voltage, which influences only the electrons. This allows one to tune the electron transport while keeping the phonons untouched. In Fig. 2, we depict the net electron heat current $\overline{J_Q^{\mathrm{el}}}$ as a function of $E_1-\mu$ for a fixed driving amplitude. We find that the heat current possesses an extremum for $E_1-\mu=0$, i.e., when the on-site energy is aligned with the Fermi energy. Interestingly enough, this extremum is a maximum for low reference temperature T_0 and turns into a minimum when the temperature exceeds a certain value. This implies that the net electron heat current is rather sensitive to the on-site energy with respect to the Fermi energy. This property thus provides an efficient way to determine experimentally the Fermi energy of the wire as an alternative to, e.g., measuring the thermopower, as proposed in Ref. [64]. For large gate variations, we find that the directed electron heat current is significantly suppressed since the wire level is far off the electron thermal energy, i.e., $E_1-\mu \gg k_{\mathrm{B}}T_0$. The directed heat current is then dominated by the phonon heat flux. As temperature is increased, the peak positions of the pumped electron heat current shift outward, away from the Fermi energy. At room temperature $T=300$ K, the peak positions are located at $E_1-\mu = \pm 0.138$ eV.

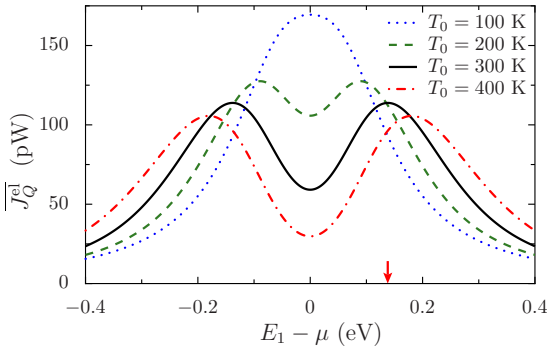

FIG. 2. (Color online) Directed electronic heat current $\overline{J_Q^{\mathrm{el}}}$ as function of on-site energy $E_1-\mu$ for different reference temperatures T_0 and temperature oscillation amplitude $A=30$ K. The arrow marks the on-site energy $E_1-\mu=0.138$ eV for which the pumped electron current assumes at temperature $T_0=300$ K its maximum. The adiabatic rocking frequency is $\Omega=3.92$ GHz.

A. Scaling behavior for small driving strengths

Figure 3 shows the total heat current $\overline{J_Q}$ as a function of the driving amplitude A for the reference temperature $T_0=300$ K and the electronic site above the Fermi level. For weak driving ($A \ll T_0$), we find $\overline{J_Q^{\mathrm{el(ph)}}} \propto A^2$ for both the electronic and the phononic contributions. This behavior can be understood from a Taylor expansion of the Fermi-Dirac distribution f and the Bose-Einstein distribution n,

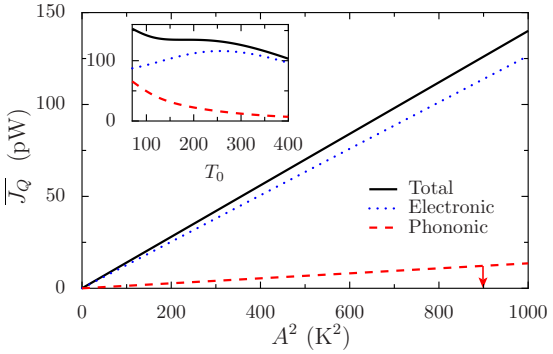

FIG. 3. (Color online) Total electronic and phononic time-averaged directed heat current $\overline{J_Q}$ as function of the squared driving amplitude A^2 with reference temperature at $T_0=300$ K for the on-site energy $E_1-\mu=0.138$ eV. The dotted blue line represents the electronic contribution; the dashed red line represents the phononic one. The inset depicts the directed heat current as a function of the reference temperature T_0 for the amplitude $A=30$ K($A^2=900$ K^2) marked by the arrow in the main panel.

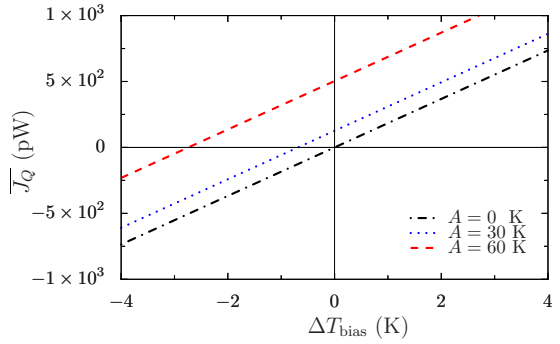

FIG. 4. (Color online) Total directed heat current $\overline{J_Q}$ as the function of static thermal bias $\Delta T_{\rm bias}$ for different driving amplitude strengths A for the temperature modulation. The reference temperature is set as $T_0=300$ K and the electronic wire level is set as $E_1-\mu=0.138$ eV.

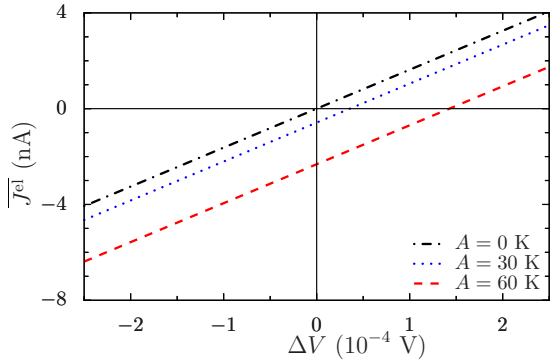

FIG. 5. (Color online) The time-averaged directed electric current $\overline{J^{\rm el}}$ as function of the static voltage bias ΔV for different temperature amplitudes A. The reference temperature is $T_0=300$ K and the electronic wire level is at $E_1-\mu=0.138$ eV.

$$\mathcal{D}(\xi,T_{\rm L})-\mathcal{D}(\xi,T_0)=\mathcal{D}(\xi,T_0+\Delta T)-\mathcal{D}(\xi,T_0)$$
$$=\mathcal{D}'(\xi,T_0)\Delta T(t)+\frac{\mathcal{D}''(\xi,T_0)}{2}[\Delta T(t)]^2+\cdots, \quad (20)$$

where $\mathcal{D}=f,n$ represents either distribution, while $\mathcal{D}'$ and $\mathcal{D}''$ denote derivatives with respect to temperature. Note that the time dependence stems solely from the temperature difference $\Delta T(t)$. After a cycle average over the driving period, the first term in the expansion vanishes owing to $\overline{\Delta T(t)}=0$. Therefore, the leading term of the heat current is of second order, i.e., $\propto\overline{[\Delta T(t)]^2}$, which yields $\overline{J_Q^{\rm el(ph)}}\propto\int_0^{2\pi/\Omega}[\Delta T(t)]^2dt\propto A^2$, as observed numerically. We also plot the directed heat current as a function of the reference temperature T_0 in the inset of Fig. 3. Upon increasing the reference temperature, the directed phonon heat current decreases monotonically. However, the emerging total heat current exhibits a relatively flat behavior in a large temperature range. This is due to the combined effect from phonons and electrons. At high temperatures, the electron contribution dominates the directed heat flow.

B. Thermal load characteristics and ratchet-induced thermoelectric voltage

Thus far, we have studied heat pumping in the absence of a static temperature bias, i.e., for $\Delta T(t)=0$. We next introduce a static thermal bias such that a thermal bias $\Delta T_{\rm bias}:=\overline{\Delta T(t)}\neq 0$ emerges. The resulting total directed heat current J_Q is depicted in Fig. 4. Within this load curve, we spot a regime with negative static thermal bias $\Delta T_{\rm bias}<0$ and positive-valued overall heat flow until $\Delta T_{\rm bias}$ reaches the stop-bias value, i.e., we find a so-called Brownian heat-ratchet effect [39,40]. This means that heat can be pumped against a thermal bias from cold to warmlike in a conventional heat pump. The width of this regime scales with the driving amplitude A^2 (cf. Fig. 4).

As can be deduced from Fig. 4, a zero-biased temperature modulation generates a finite net heat flow at zero-temperature bias similar to the heat flow that would be induced by a static thermal bias. Near equilibrium, i.e., within the linear-response regime, Onsager symmetry relations for conjugated transport quantities are expected to hold. Therefore, the adiabatic temperature modulations are expected to induce an *electric current* as well. This net adiabatic electric pump current can be obtained by means of the cycle-averaged Landauer expression

$$\overline{J^{\rm el}}=\frac{\Omega}{2\pi}\int_0^{2\pi/\Omega}dt\frac{e}{h}\int d\varepsilon\mathcal{T}(\varepsilon)[f(\varepsilon,T_{\rm L})-f(\varepsilon,T_{\rm R})]. \quad (21)$$

We, in addition, apply a net static voltage bias ΔV. Figure 5 depicts the net electric current-voltage characteristics $\overline{J^{\rm el}}(\Delta V)$ in the presence of an unbiased temperature modulation while, importantly, no external thermal bias is applied. For a finite range of positive bias voltages $\Delta V>0$, the net electric current is negative, i.e., the system acts as an "electron pump."

When the voltage bias ΔV assumes a certain value, namely, the so-called stop voltage $\Delta V_{\rm stop}$, the bias-induced current and the driving-induced current compensate each other. This value can be interpreted as a sole heat-ratchet-induced thermopower. We term this phenomenon *ratchet Seebeck effect*. Knowingly, the usual thermopower (Seebeck coefficient) is defined by means of the change in induced voltage per unit change in applied temperature bias under conditions of zero electric current [67]. Here, in the absence of a net thermal bias, we introduce instead the Grüneisen-like relation $\gamma=|\Delta V_{\rm eff}/\overline{J^{\rm el}}(\Delta V=0)|$, where $\Delta V_{\rm eff}$ denotes the effective static voltage bias, which yields the *identical* electric current $\overline{J^{\rm el}}(\Delta V=0)$ as generated by our imposed temperature modulation. We find that this effective voltage bias precisely matches the above-mentioned stop voltage, i.e., $\Delta V_{\rm eff}=-\Delta V_{\rm stop}$. Due to the linear $\overline{J^{\rm el}}-\Delta V$ characteristics, as evidenced with Fig. 5, the ratchet-induced Grüneisen constant γ is independent of the amplitude of the temperature modulation. In Figs. 6(a) and 6(b), we depict the reciprocal of γ as a function of varying reference temperature T_0 [Fig. 6(a)] and varying on-site energy $E_1-\mu$, respectively [Fig. 6(b)]. We detect a resonancelike dependence $1/\gamma$ as a function the reference temperature T_0, while it decreases monotonically with increasing on-site energy E_1. Note also that

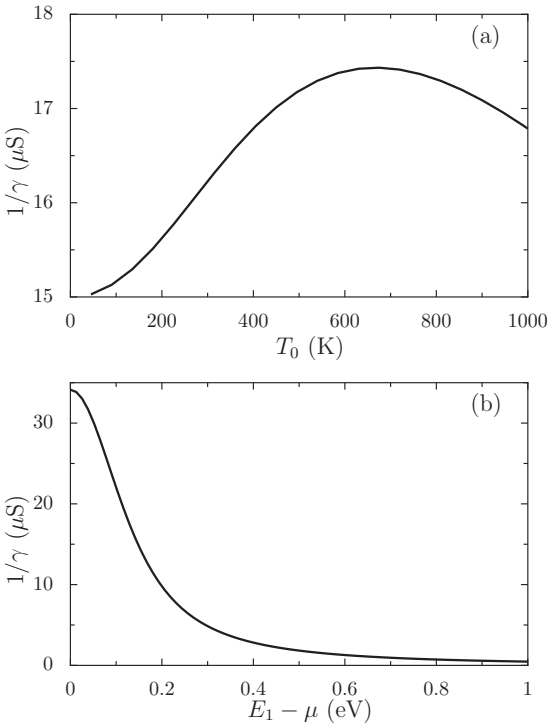

FIG. 6. The reciprocal of the Grüneisen-like constant $1/\gamma$ as the function of (a) reference temperature T_0 with $E_1-\mu=0.138$ eV and (b) on-site energy $E_1-\mu$ with $T_0=300$ K. For both cases, the driving amplitude is set as $A=30$ K.

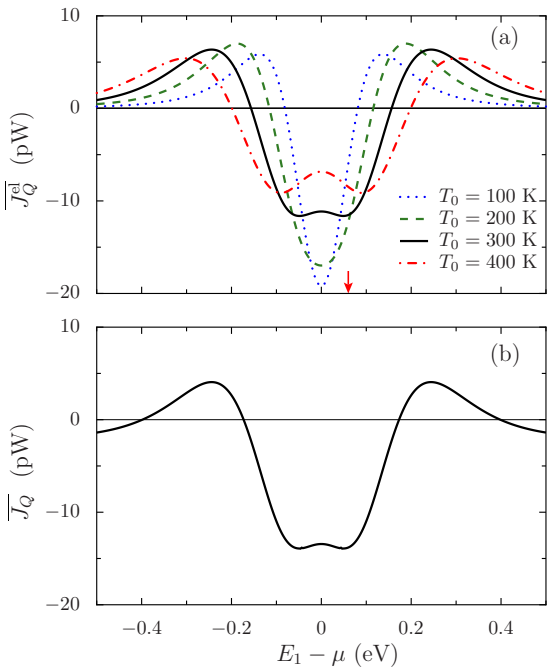

FIG. 7. (a) (Color online) Directed electron heat current $\overline{J_Q^{el}}$ as function of the wire level $E_1-\mu$ for various reference temperatures T_0. The driving parameters are $A_1=A_2=30$ K and harmonic mixing phase lag $\varphi=0$. (b) Total net heat current $\overline{J_Q}$ as function of the wire level $E_1-\mu$ for reference temperature $T_0=300$ K and amplitudes $A_1=A_2=30$ K, with harmonic mixing phase lag $\varphi=0$.

this Grüneisen parameter γ is a symmetric function of $E_1-\mu$.

IV. TEMPERATURE ROCKING IN BOTH LEADS: PUMPING HEAT BY DYNAMICAL SYMMETRY BREAKING

We next consider temperature modulations applied to both leads in the absence of a thermal bias. The temperature driving consists of a contribution with frequency Ω and a second harmonic with frequency 2Ω. This entails a dynamical symmetry breaking, namely, harmonic mixing [43–47]. The time-dependent lead temperatures are chosen as

$$T_{L,R} = T_0 \pm [A_1 \cos(\Omega t) + A_2 \cos(2\Omega t + \varphi)], \qquad (22)$$

such that again $\overline{T_L(t)}=\overline{T_R(t)}=T_0$ and $\Delta T(t) = 2[A_1 \cos(\Omega t)+A_2 \cos(2\Omega t+\varphi)]$. Then the average temperature bias vanishes irrespective of the phase lag φ.

In Fig. 7(a), we depict the resulting electron heat current $\overline{J_Q^{el}}$ as a function of the on-site energy $E_1-\mu$ for various reference temperatures T_0. At low temperatures, the net electron heat current exhibits a minimum at the Fermi energy. With increasing reference temperature T_0, this minimum develops into a local maximum with two local minima in its vicinity. The arrow in Fig. 7(a) marks the minimum at $E_1-\mu=0.049$ eV for $T_0=300$ K. It is interesting that the direction of the net electron heat current can be controlled by the gate voltage. For an electron wire level close to the Fermi energy, the directed electron heat current is negative. Upon tuning the gate voltage, the heat current undergoes a reversal and becomes positive when $E_1-\mu$ is larger than 0.15 eV (at reference temperature $T_0=300$ K) and eventually approaches zero again for large detuning.

Figure 7(b) shows the corresponding sum of electron and phonon heat flow, i.e., the net heat current $\overline{J_Q}$ as a function of wire level $E_1-\mu$. The net phonon heat current $\overline{J_Q^{ph}}$ is negative for these parameters (not depicted) and is not sensitive to the gate voltage. As a consequence, $\overline{J_Q}$ exhibits *multiple current reversals* as the on-site energy $E_1-\mu$ increases. For small values of $E_1-\mu$, i.e., close to the Fermi surface, both the electron and the phonon heat fluxes are negative and in phase with the driving. There the absolute value of the total heat current assumes its maximum (at which the heat current is negative). For intermediate values of $E_1-\mu$, the direction of total net current $\overline{J_Q}$ is reversed due to the dominating positive contribution of the electrons. At even larger values of $E_1-\mu$, the electron heat current almost vanishes, so that the total heat current is dominated by the negative-valued contribution of the phonons. In the limit of large $E_1-\mu$, we find saturation at a negative value.

We also study with Fig. 8 the net electron and phonon heat current as a function of driving amplitudes A_1, A_2, and of the relative phase φ. Both contributions scale as $\overline{J_Q^{el/ph}} \propto A_1^2 A_2 \cos(\varphi)$, which implies that they can be manipulated simultaneously. This behavior can be understood by again expanding the Fermi-Dirac distribution f and the Bose-Einstein distribution n in ΔT around the average temperature T_0,

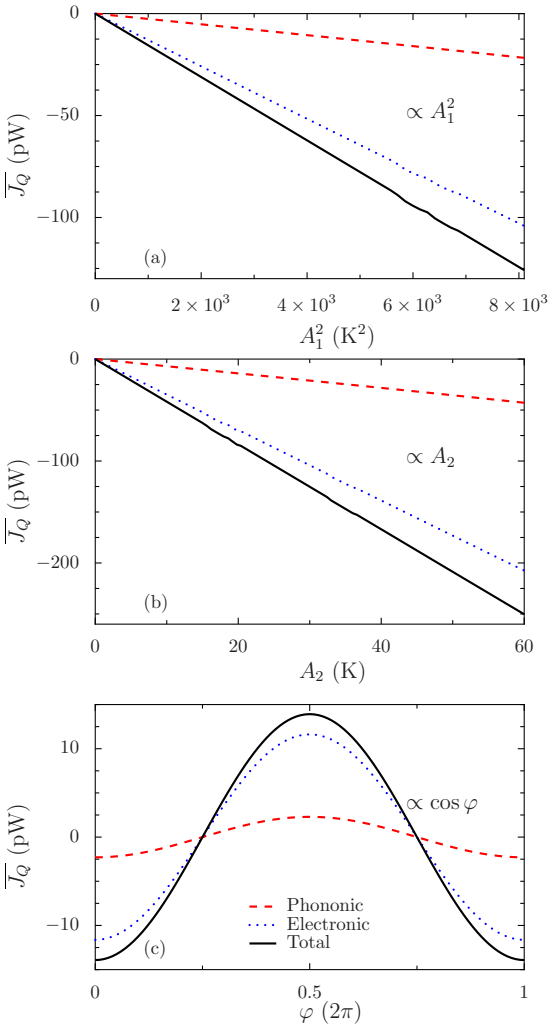

FIG. 8. (Color online) Heat current $\overline{J_Q}$ as function of (a) fundamental driving strength A_1, where $A_2=30$ K and $\varphi=0$ and (b) as function of the second-harmonic amplitude A_2, where $A_1=90$ K and $\varphi=0$. (c) Dependence on the relative phase φ for $A_1=A_2=30$ K. The reference temperature is $T_0=300$ K, while the wire level is $E_1-\mu=0.049$ eV.

$$\mathcal{D}(\xi,T_L)-\mathcal{D}(\xi,T_R)=\mathcal{D}(\xi,T_0+\Delta T/2)-\mathcal{D}(\xi,T_0-\Delta T/2)$$
$$=\mathcal{D}'(\xi,T_0)\Delta T(t)+\frac{\mathcal{D}'''(\xi,T_0)}{24}[\Delta T(t)]^3$$
$$+\cdots, \tag{23}$$

where $\mathcal{D}=f,n$ represents the distribution function for either the electrons or for the phonons, respectively. The terms of even order in ΔT vanish owing to the antisymmetric temperature modulation. Thus, the heat currents are governed by the time average of the odd powers $[\Delta T(t)]^{2n+1}$ with $n>1$ since $\overline{\Delta T}=0$. It can be easily verified that all these time-averaged odd moments vanish if either amplitude A_1 or A_2 vanishes.

Note that the lowest-order contribution, i.e., the third moment reads as $\overline{[\Delta T(t)]^3}=8A_1^2A_2\cos(\varphi)$. Thus, for small driving amplitudes $A_1,A_2\ll T_0$, this explains the proportionality to $A_1^2A_2\cos(\varphi)$ of the numerical results depicted in Figs. 8(a)–8(c). The proportionality to $\cos(\varphi)$ [see Fig. 8(c)] is even more robust than expected because the cycle-averaged 5th and 7th moments are proportional to $\cos(\varphi)$ as well, i.e., $\overline{[\Delta T(t)]^5},\overline{[\Delta T(t)]^7}\propto\cos(\varphi)$. This behavior can be employed for a sensitive control of the heat current. The direction of the heat current can be reversed by merely adjusting the relative phase φ between the two harmonics. Note that for the parameters used in the figure, the net electron heat current $\overline{J_Q^{\rm el}}$ exceeds the net phonon heat current $\overline{J_Q^{\rm ph}}$ roughly by a factor 5.

V. CONCLUSIONS

We have demonstrated the possibility of steering heat across a gated two-terminal molecular junction, owing to lead temperatures that undergo adiabatic, unbiased, and time-periodic modulations. In a realistic molecule, the heat flow is carried by the electrons as well as by the phonons. Our study considers both contributions. Two scenarios of temperature modulations have been investigated, namely, directed heat flow induced (i) by periodic temperature manipulation in one connecting lead and (ii) by a temperature modulation that includes a contribution oscillating with twice the fundamental frequency. In both cases, we predict a finite heat current, which is related to dynamical breaking of reflection symmetry. A necessary ingredient is the nonlinearity of the initial electron and phonon distributions, which is manifested in the Fermi-Dirac distribution and the Bose-Einstein distribution. The first scenario yields sizable heat currents proportional to the squared amplitude of the temperature modulation. The resulting heat flow occurs in the absence of a static thermal bias. We also studied heat pumping against an external static thermal bias and computed the corresponding thermal heat-current load characteristics. Moreover, the ratchet heat flow in turn generates an electric current. This ratchet heat current induces a ratchet-induced effective thermopower (see in Fig. 5).

When the asymmetry is induced by temperature rocking at both leads, the resulting net heat current becomes smaller. This is so because the leading-order time-averaged heat flow now starts out with the third moment of the driving amplitude. The benefit of this second scenario is the possibility of controlling efficiently both the magnitude and the sign of the net heat flow. For example, the direction of the heat current can be readily reversed via the gate voltage or the relative phase between two temperature modulations that are harmonically mixed. When adjusting the gate voltage, the directed heat current experiences multiple reversals. The directed heat flow is even up to seventh order in the amplitude proportional to the cosine of the phase between the fundamental frequency and the second harmonic. This allows robust control even for relatively large temperature amplitudes.

These theoretical findings may inspire experimental efforts to steer heat in a controlled manner across a molecular junction as well as the development of concepts for measuring system parameters via their impact on the heat current. For example, as elucidated in Sec. III, the Fermi energy can be sensitively gauged in this way.

ACKNOWLEDGMENTS

The authors like to thank W. Häusler for his comments on this work. The work has been supported by the German Excellence Initiative via the "Nanosystems Initiative Munich" (NIM) (P.H.), the German-Israel-Foundation (GIF) (N.L. and P.H.), and the DFG priority program SPP 1243 "quantum transport at the molecular scale" (F.Z., P.H., and S.K.).

APPENDIX: THE DERIVATION OF PHONON TRANSMISSION (18)

We derive the phonon transmission coefficient of Eq. (18) along the lines of Ref. [55]. Starting with Eq. (33) of that work and assuming symmetric coupling, i.e., $\gamma^{L}_{k,k'}(\omega_0)=\gamma^{R}_{k,k'}(\omega_0)=\gamma_{k,k'}(\omega_0)$, Eq. (33) of Ref. [55] can be simplified to read as

$$[\omega_k^2-\omega_0^2+2i\omega_0\gamma_{k,k}(\omega_0)]A_k(\omega_0) + i\omega_0\sum_{k'\neq k}\sqrt{\frac{\omega_k}{\omega_{k'}}}2\gamma_{k,k'}(\omega_0)A_{k'}(\omega_0) = \sqrt{\frac{\omega_k}{\omega_0}}V_{0,k}a_0^{\dagger}, \tag{A1}$$

where ω_0 is a dummy variable.

Since we only consider one phonon mode, i.e., $k=1$. The second term in the left-hand side of the last equation vanishes such that

$$[\omega_1^2-\omega_0^2+2i\omega_0\gamma_{1,1}(\omega_0)]A_1(\omega_0)=\sqrt{\frac{\omega_1}{\omega_0}}V_{0,1}a_0^{\dagger}. \tag{A2}$$

Substituting Eq. (46) of Ref. [55], i.e.,

$$A_k(\omega_0)=\overline{A_k}(\omega_0)V_{0,k}a_0^{\dagger}\sqrt{\frac{\omega_k}{\omega_0}} \tag{A3}$$

into Eq. (A2), we find

$$\overline{A_1}(\omega_0)=\frac{1}{\omega_1^2-\omega_0^2+2i\omega_0\gamma_{1,1}(\omega_0)}. \tag{A4}$$

For one phonon mode, the phonon transmission is defined from Eq. (48) in [55]. However, this definition is $1/2\pi$ times smaller than the commonly used definition of Refs. [53,56]. With the commonly used definition, the phonon transmission can be expressed as

$$\mathcal{T}(\omega)=4\omega^2\gamma_{1,1}^2(\omega)|\overline{A_1}(\omega)|^2. \tag{A5}$$

Substituting Eq. (A4) into the last equation and omitting the subscript in $\gamma_{1,1}$, we obtain

$$\mathcal{T}(\omega)=\frac{4\omega^2\gamma^2(\omega)}{(\omega_1^2-\omega^2)^2+4\omega^2\gamma^2(\omega)}, \tag{A6}$$

which is the phonon transmission (18) employed in the main text.

[1] A. Nitzan and M. A. Ratner, Science **300**, 1384 (2003).
[2] *Molecular Nanoelectronics*, edited by M. A. Reed and T. Lee (American Scientific, Stevenson Ranch, CA, 2003).
[3] P. Hänggi, M. Ratner, and S. Yaliraki, Chem. Phys. **281**, 111 (2002).
[4] S. Kohler, J. Lehmann, and P. Hänggi, Phys. Rep. **406**, 379 (2005).
[5] N. J. Tao, Nat. Nanotechnol. **1**, 173 (2006).
[6] M. A. Reed and J. M. Tour, Sci. Am. (Int. Ed.) **282** (6), 86 (2000).
[7] P. J. Kuekes, D. R. Stewart, and R. S. Williams, J. Appl. Phys. **97**, 034301 (2005).
[8] C. Zhang, M.-H. Du, H.-P. Cheng, X.-G. Zhang, A. E. Roitberg, and J. L. Krause, Phys. Rev. Lett. **92**, 158301 (2004).
[9] J. Lehmann, S. Camalet, S. Kohler, and P. Hänggi, Chem. Phys. Lett. **368**, 282 (2003).
[10] J. Lehmann, S. Kohler, V. May, and P. Hänggi, J. Chem. Phys. **121**, 2278 (2004).
[11] G.-Q. Li, M. Schreiber, and U. Kleinekathöfer, EPL **79**, 27006 (2007).
[12] I. Franco, M. Shapiro, and P. Brumer, Phys. Rev. Lett. **99**, 126802 (2007).
[13] S. Kohler and P. Hänggi, Nat. Nanotechnol. **2**, 675 (2007).
[14] Z. Q. Yang, N. D. Lang, and M. Di Ventra, Appl. Phys. Lett. **82**, 1938 (2003).
[15] A. Ghosh, T. Rakshit, and S. Datta, Nano Lett. **4**, 565 (2004).
[16] F. Jiang, Y. X. Zhou, H. Chen, R. Note, H. Mizuseki, and Y. Kawazoe, J. Chem. Phys. **125**, 084710 (2006).
[17] K. Xiao, Y. Liu, T. Qi, W. Zhang, F. Wang, J. Gao, W. Qiu, Y. Ma, G. Cui, S. Chen, X. Zhan, G. Yu, J. Qin, W. Hu, and D. Zhu, J. Am. Chem. Soc. **127**, 13281 (2005).
[18] Y. Sun, Y. Liu, and D. Zhu, J. Mater. Chem. **15**, 53 (2005).
[19] B. Xu, X. Xiao, X. Yang, L. Zang, and N. Tao, J. Am. Chem. Soc. **127**, 2386 (2005).
[20] L. Wang and B. Li, Phys. World **21**, 27 (2008).
[21] M. Terraneo, M. Peyrard, and G. Casati, Phys. Rev. Lett. **88**, 094302 (2002).
[22] B. Li, L. Wang, and G. Casati, Phys. Rev. Lett. **93**, 184301 (2004).
[23] D. Segal and A. Nitzan, Phys. Rev. Lett. **94**, 034301 (2005).
[24] B. Hu, L. Yang, and Y. Zhang, Phys. Rev. Lett. **97**, 124302 (2006).
[25] M. Peyrard, Europhys. Lett. **76**, 49 (2006).
[26] N. Yang, N. Li, L. Wang, and B. Li, Phys. Rev. B **76**, 020301(R) (2007).
[27] D. Segal, Phys. Rev. Lett. **100**, 105901 (2008).
[28] B. Li, L. Wang, and G. Casati, Appl. Phys. Lett. **88**, 143501 (2006).
[29] W. C. Lo, L. Wang, and B. Li, J. Phys. Soc. Jpn. **77**, 054402 (2008).
[30] L. Wang and B. Li, Phys. Rev. Lett. **99**, 177208 (2007).
[31] L. Wang and B. Li, Phys. Rev. Lett. **101**, 267203 (2008).
[32] C. W. Chang, D. Okawa, A. Majumdar, and A. Zettl, Science **314**, 1121 (2006).

[33] R. Scheibner, M. König, D. Reuter, A. D. Wieck, C. Gould, H. Buhmann, and L. W. Molenkamp, New J. Phys. **10**, 083016 (2008).
[34] P. Reimann, R. Bartussek, R. Häussler, and P. Hänggi, Phys. Lett. A **215**, 26 (1996).
[35] R. D. Astumian and P. Hänggi, Phys. Today **55**(11), 33 (2002).
[36] P. Hänggi, F. Marchesoni, and F. Nori, Ann. Phys. **14**, 51 (2005).
[37] P. Reimann and P. Hänggi, Appl. Phys. A: Mater. Sci. Process. **75**, 169 (2002).
[38] P. Hänggi and F. Marchesoni, Rev. Mod. Phys. **81**, 387 (2009).
[39] N. Li, P. Hänggi, and B. Li, EPL **84**, 40009 (2008).
[40] N. Li, F. Zhan, P. Hänggi, and B. Li, Phys. Rev. E **80**, 011125 (2009).
[41] M. Rey, M. Strass, S. Kohler, P. Hänggi, and F. Sols, Phys. Rev. B **76**, 085337 (2007).
[42] L. Arrachea, M. Moskalets, and L. Martin-Moreno, Phys. Rev. B **75**, 245420 (2007).
[43] J. Luczka, R. Bartussek, and P. Hänggi, Europhys. Lett. **31**, 431 (1995).
[44] P. Hänggi, R. Bartussek, P. Talkner, and J. Luczka, Europhys. Lett. **35**, 315 (1996).
[45] I. Goychuk and P. Hänggi, Europhys. Lett. **43**, 503 (1998).
[46] S. Flach, O. Yevtushenko, and Y. Zolotaryuk, Phys. Rev. Lett. **84**, 2358 (2000).
[47] S. Denisov, S. Flach, A. A. Ovchinnikov, O. Yevtushenko, and Y. Zolotaryuk, Phys. Rev. E **66**, 041104 (2002).
[48] M. Galperin, M. A. Ratner, and A. Nitzan, J. Phys.: Condens. Matter **19**, 103201 (2007).
[49] D. Segal and A. Nitzan, J. Chem. Phys. **122**, 194704 (2005).
[50] D. Segal, Phys. Rev. B **73**, 205415 (2006).
[51] U. Sivan and Y. Imry, Phys. Rev. B **33**, 551 (1986).
[52] X. Zheng, W. Zheng, Y. Wei, Z. Zeng, and J. Wang, J. Chem. Phys. **121**, 8537 (2004).
[53] L. G. C. Rego and G. Kirczenow, Phys. Rev. Lett. **81**, 232 (1998).
[54] A. Ozpineci and S. Ciraci, Phys. Rev. B **63**, 125415 (2001).
[55] D. Segal, A. Nitzan, and P. Hänggi, J. Chem. Phys. **119**, 6840 (2003).
[56] J.-S. Wang, J. Wang, and J. T. Lü, Eur. Phys. J. B **62**, 381 (2008).
[57] J. Lee, A. O. Govorov, and N. A. Kotov, Angew. Chem., Int. Ed. **44**, 7439 (2005).
[58] R. H. M. Groeneveld, R. Sprik, and A. Lagendijk, Phys. Rev. B **51**, 11433 (1995).
[59] N. Del Fatti, C. Voisin, M. Achermann, S. Tzortzakis, D. Christofilos, and F. Valleé, Phys. Rev. B **61**, 16956 (2000).
[60] R. Knorren, K. H. Bennemann, R. Burgermeister, and M. Aeschlimann, Phys. Rev. B **61**, 9427 (2000).
[61] P. J. van Hall, Phys. Rev. B **63**, 104301 (2001).
[62] J. P. Girardeau-Montaut, M. Afif, C. Girardeau-Montaut, S. D. Moustaïzis, and N. Papadogiannis, Appl. Phys. A: Mater. Sci. Process. **62**, 3 (1996).
[63] M. van Kampen, J. T. Kohlhepp, W. de Jonge, B. Koopmans, and R. Coehoorn, J. Phys.: Condens. Matter **17**, 6823 (2005).
[64] M. Paulsson and S. Datta, Phys. Rev. B **67**, 241403(R) (2003).
[65] J. Grunenberg, Angew. Chem., Int. Ed. **40**, 4027 (2001).
[66] Z. Wang, J. A. Carter, A. Lagutchev, Y. K. Koh, N. Seong, D. G. Cahill, and D. D. Dlott, Science **317**, 787 (2007).
[67] H. B. Callen, *Thermodynamics and an Introduction to Thermostatics*, 2nd ed. (Wiley, New York, 1985), see Secs. 14.5–14.9 therein.